BBA - General Subjects 1864 (2020) 129533

Contents lists available at ScienceDirect

BBA - General Subjects

journal homepage: www.elsevier.com/locate/bbagen

Metformin attenuates adhesion between cancer and endothelial cells in chronic hyperglycemia by recovery of the endothelial glycocalyx barrier

Marta Targosz-Korecka[a,*], Katarzyna Ewa Malek-Zietek[a], Damian Kloska[b], Zenon Rajfur[c], Ewa Łucja Stepien[d], Anna Grochot-Przeczek[b,**], Marek Szymonski[a]

[a] Department of Physics of Nanostructures and Nanotechnology, Faculty of Physics, Astronomy and Applied Computer Science, Jagiellonian University, Krakow, Poland
[b] Department of Medical Biotechnology, Faculty of Biochemistry, Biophysics and Biotechnology, Jagiellonian University, Krakow, Poland
[c] Department of Molecular and Interfacial Biophysics, Faculty of Physics, Astronomy and Applied Computer Science, Krakow, Poland
[d] Department of Medical Physics, Faculty of Physics, Astronomy and Applied Computer Science, Jagiellonian University, Krakow, Poland

ARTICLE INFO

Keywords:
Nanoindentation
AFM
Single-cell force spectroscopy
Cancer cells
Endothelial cells
Glycocalyx
Metformin

ABSTRACT

Background: Epidemiologic studies suggest that diabetes is associated with an increased risk of cancer. Concurrently, clinical trials have shown that metformin, which is a first-line antidiabetic drug, displays anticancer activity. The underlying mechanisms for these effects are, however, still not well recognized.
Methods: Methods based on atomic force microscopy (AFM) were used to directly evaluate the influence of metformin on the nanomechanical and adhesive properties of endothelial and cancer cells in chronic hyperglycemia. AFM single-cell force spectroscopy (SCFS) was used to measure the total adhesion force and the work of detachment between EA.hy926 endothelial cells and A549 lung carcinoma cells. Nanoindentation with a spherical AFM probe provided information about the nanomechanical properties of cells, particularly the length and grafting density of the glycocalyx layer. Fluorescence imaging was used for glycocalyx visualization and monitoring of *E*-selectin and ICAM-1 expression.
Results: SCFS demonstrated that metformin attenuates adhesive interactions between EA.hy926 endothelial cells and A549 lung carcinoma cells in chronic hyperglycemia. Nanoindentation experiments, confirmed by confocal microscopy imaging, revealed metformin-induced recovery of endothelial glycocalyx length and density. The recovery of endothelial glycocalyx was correlated with a decrease in the surface expression of *E*-selectin and ICAM-1.
Conclusion: Our results identify metformin-induced endothelial glycocalyx restoration as a key factor responsible for the attenuation of adhesion between EA.hy926 endothelial cells and A549 lung carcinoma cells.
General significance: Metformin-induced glycocalyx restoration and the resulting attenuation of adhesive interactions between the endothelium and cancer cells may account for the antimetastatic properties of this drug.

1. Background

Metformin is a first-line antidiabetic drug that decreases blood glucose concentration and improves insulin sensitivity. Although the mechanism of its activity is still not well recognized [1], its predominant effect on glucose metabolism is mostly attributed to direct inhibition of mitochondrial respiratory complex I in hepatocytes, suppression of gluconeogenesis and augmentation of glycolysis. A metformin-induced drop in the ATP/AMP ratio may also activate AMPK, eventually disrupting gluconeogenesis and lipogenesis gene expression [2]. Experimental studies have shown that metformin, beyond its primary action, exerts a protective effect on endothelial cells (ECs) and the cardiovascular system. It prevents EC apoptosis [3] and premature senescence [4], enhances activation of endothelial nitric oxide synthase (eNOS) [5,6] and attenuates overexpression of adhesion molecules on ECs [6]. Metformin reduces infarct size [7] and counteracts endoplasmic reticulum stress, oxidative stress and vasorelaxation impairment [5]. It is suggested that these effects can also be achieved

Abbreviations: AFM, atomic force microscopy; EC, endothelial cell; SCFS, single-cell force spectroscopy; T2D, type 2 diabetes

* Correspondence to: M. T. Korecka, Department of Physics of Nanostructures and Nanotechnology, Faculty of Physics, Astronomy and Applied Computer Science, Jagiellonian University, 30-348 Krakow, Poland.
** Correspondence to: A. G. Przeczek, Department of Medical Biotechnology, Faculty of Biochemistry, Biophysics and Biotechnology, Jagiellonian University, 30-387 Krakow, Poland.
E-mail addresses: marta.targosz-korecka@uj.edu.pl (M. Targosz-Korecka), anna.grochot-przeczek@uj.edu.pl (A. Grochot-Przeczek).

https://doi.org/10.1016/j.bbagen.2020.129533
Received 19 July 2019; Received in revised form 30 December 2019; Accepted 13 January 2020
Available online 15 January 2020

independently of glucose and lipid metabolism [5]. Moreover, treatment of rodents with metformin was shown to extend their lifespan [8,9], but there are also studies contradicting these findings [10,11]. The clinical data demonstrate beneficial effects of metformin in patients with type 2 diabetes (T2D), as it lowers the risk of all-cause mortality [12,13]. However, its impact on the risk of cardiovascular diseases remains uncertain, especially in nondiabetic patients [1,14].

Clinical trials documented that T2D is associated with an increased risk of cancer development and worse disease outcome [15,16]. Hyperglycemia boosts cancer cell metabolism and promotes their proliferation, invasiveness and metastasis [17]. Moreover, hyperinsulinemia may contribute to cancer progression through insulin receptor and insulin-like growth factor signaling [16]. Long-term clinical studies indicate that metformin may exert anticancer properties. It was shown to reduce the risk of cancer and decrease cancer mortality in patients with T2D [18–21]. The detailed mechanisms are not entirely clear, however. Molecularly, the anticancer activity of metformin can be related to both AMPK-dependent and AMPK-independent effects, including mainly mTOR and IGF-1 signaling inhibition (broadly reviewed by Pernicova & Korbonits [22]). Furthermore, metformin exerts anti-angiogenic properties, which may also contribute to the reduction of tumor growth [23]. In our study, we focused on the antimetastatic potential of metformin, the mechanism of which has been poorly understood thus far.

Cancer metastasis is a multiphase process, with a crucial step of crossing the endothelial barrier by the cancer cell, involving direct interactions of the cancer cell and the endothelium [24]. Such cell-to-cell interactions, similar to leukocyte-endothelial interactions, are regulated by the glycocalyx, a protective polysaccharide layer forming a physical and functional barrier, found on the apical part of the endothelium [25]. In hyperglycemic conditions, the endothelial glycocalyx layer is reduced [26], which may facilitate the adhesion of circulating cells to the activated endothelium [27]. In accordance, our recent study shows that short-term hyperglycemia induces changes in both the mechanical and structural properties of the endothelial glycocalyx, which in turn modulates the adhesion of cancer cells to the endothelium [28].

Atomic force microscopy (AFM) is a useful tool for studying the nanomechanical and adhesive properties of cells due to its ability to control interactions between two objects within a range of nanonewton (nN) forces. Using single-cell force spectroscopy (SCFS), it is possible to investigate adhesive interactions between single cells directly [29,30]. Moreover, the AFM nanoindentation method enables the measurement of the length and density of the glycocalyx layer as well as the elastic properties of the cell body. In this work, we used AFM methods to verify whether metformin can attenuate the adhesion of cancer cells to the endothelium and, if so, whether it can be achieved by regulating endothelial glycocalyx properties.

2. Methods

2.1. Cell culture

Human lung carcinoma A549 (ATCC, UK) cells were cultured in F-12 K medium (Cat. No. 30–2004, ATCC) supplemented with 10% fetal bovine serum (FBS, Cat. No. 10082–147, Invitrogen). EA.hy926 (ATCC), immortalized human umbilical vein endothelial cells, were grown in Dulbecco's modified Eagle's medium with 25 mM glucose (high glucose, HG) (Cat. No. 30–2002, ATCC), 10% FBS (Cat. No. 10082–147, Invitrogen) and 2% HAT supplement (Cat. No. 21060–017, Invitrogen). The cells were maintained in standard conditions at 37 °C, 5% CO_2, and 95% humidity.

2.2. Experimental scheme

EA.hy926 cells were seeded in DMEM HG supplemented with 10% FBS and 2% HAT at a density of 10^4 cells/mL on sticky-slides I 0.6 (Cat. No. 80188, IBIDI) covered with fibronectin and were kept in static conditions for 24 h to allow their attachment. After this time, slides were inserted into the fluidic unit (IBIDI pump system for simulation of blood vessels), and the cells were subjected to a laminar shear stress of 20 dyn/cm^2 for 48 h (Fig. S1A–C). To prepare A549 cells for the AFM measurements, the cells were plated in F-12 K medium supplemented with 10% FBS and 25 mM glucose. Both cell lines were treated with metformin either for 72 h (short-term) or additionally pretreated for 12 days (long-term) (Fig. S1D). Heparinase (1000 U/mL, Sigma) was added to the cells for the last 30 min of incubation with metformin (short-term experimental scheme).

2.3. AFM study of the nanomechanics and cell-to-cell adhesion

All AFM measurements were performed using a NanoWizard 3 NanoScience AFM commercial instrument (JPK Instruments, Germany). The nanoindentation measurements with a spherical (colloidal) probe (Novascan, USA) were used to detect the endothelial glycocalyx and determine the apparent elastic modulus of ECs (Fig. S2A). We used a sphere probe with a diameter of 4.5 μm attached to the cantilever with a spring constant of 0.02 N/m. Force–distance curves were obtained with an indentation velocity of 0.7 μm/s and a maximal force of 1 nN. The measurements were performed on living cells in Hanks' Balanced Salt Solution (H8264, Sigma-Aldrich) supplemented with 25 mM glucose and 1% FBS, with or without 10 μM metformin. Experiments were conducted on the top of ECs (central part; deformation of the cell up to 10% of the cell height was applied to avoid the potential influence of the underlying nucleus).

To determine glycocalyx parameters as well as the elastic modulus, we used a procedure proposed by Sokolov et al. [31] (Fig. S2B). In the Sokolov's model, it is assumed that the surface of the cell is not homogenous, and it consists of an inner elastic body covered with the outer cellular brush. Such a brush model implies that a well-defined spherical AFM probe at first indents the cellular brush (squeezes the brush), and next the probe indents the cell body. Therefore, non-linear deformation of the brush could be analyzed by a fit based on the Alexander-de Gennes' theory of polymer brushes [31,32]. Following the procedure described in our recent paper [28], initially the Hertz model was fitted to the part of the curve close to the maximal force load (blue curve), for which the glycocalyx is assumed to be almost squeezed. Next, the brush model was fitted to the F(h) curve (Fig. S2B inset) to calculate the length and grafting density of the glycocalyx layer. The grey area shows a range of fit (Fig. S2B inset). Additionally, the assumption of total squeezing of the glycocalyx layer has been verified experimentally by measuring the dependence of the elastic modulus on the applied load (see Fig. S2C in Supplementary Information). For load forces higher than 0.8 nN, the saturation of the elastic modulus dependence on the applied force was observed.

Single-cell force spectroscopy (SCFS) study was conducted to evaluate the interactions between the A549-EA.hy926 system (see Supplementary Information Fig. S3A). Adhesive measurements were carried out using a V-shaped cantilever with a spring constant of 0.01 N/m (MLCT O-10, Bruker). The methodology of SCFS measurements was described in detail in our previous work [28]. In brief, tipless cantilevers were covered with 50 μg/mL fibronectin (Sigma-Aldrich) and were stored in PBS. To immobilize a single cancer cell on the cantilever, a functionalized cantilever was brought into contact for 30 s with a loosely bound cell. Next, a cantilever with a single cancer cell was immediately taken for measurements. The adhesive interactions between A549 and EA.hy926 cells were measured in Hanks' Balanced Salt Solution (H8264, Sigma-Aldrich) supplemented with 25 mM glucose and 1% FBS, with or without 10 μM metformin. Experiments were conducted on the central part of the cell. Fig. S3B presents an exemplary graph of a typical force-distance F(Z) curve obtained during the adhesive study. Measurement began when the cantilever with attached living cancer was separated from ECs, and it approached the

monolayer of EA.hy926 cells at 1.9 μm/s until a preset contact force of 1.4 nN was reached (grey curve). After a defined contact time of 2 s, the cantilever was retracted at a velocity of 1.9 μm/s (black curve). The contact time and contact force were controlled experimentally (see Supplementary Information Fig. S3C and S3D). It proceeded as follows: at first, the adhesion force was measured as a function of the contact time or the contact force. Next, based on these measurements, the values of contact time and contact force were chosen from the range, for which the adhesion force did not change significantly. The total adhesion force (F_d) and work of detachment (W_d) were extracted from the retraction curve using the JPK data processing software. The total adhesion force F_d was described as the maximal force required to detach A549 cells from EA.hy926 cells and was calculated as the outermost point on the adhesive curve. It should be noted that the F_d parameter characterizes only the net adhesive interactions between two cells, without discrimination of specific and non-specific interactions. The work of detachment is presented as the area between the contour of the retraction curve and the baseline. We defined the rupture events as unbinding events occurring for a small cell-cell separation distance, which are associated with the breakage of bonds involving surface molecules. The number of rupture events means the number of unbinding events detected per single curve.

2.4. AFM imaging

The AFM imaging was performed using V-shaped gold-coated cantilevers (MLCT, Veeco Probes, Camarillo, CA, USA) with a nominal spring constant of 0.01 N/m. All experiments were performed with nonfixed cells in Hanks' Balanced Salt Solution (H8264, Sigma-Aldrich) supplemented with 25 mM glucose and 1% FBS. Images (256 × 256 pixels) were obtained at a scan size of 60 × 60 μm^2 at a scan rate of 0.4 Hz. Between 10 and 15 images of cells were obtained for each sample.

2.5. Phalloidin staining

For each fluorescence experiment, ECs were grown on 24-well plates and stimulated with 10 μM metformin for 72 h or 360 h. Before staining, the culture medium was removed from wells, the cells were rinsed with warm PBS and then were fixed with 3.6% formaldehyde (Sigma) for 10 min at room temperature. Next, the cells were rinsed three times with warm buffer and permeabilized with 0.1% Triton X (Invitrogen-Thermo Fisher) for 4 min, followed by blocking in PBS containing 1% BSA (Invitrogen-Thermo Fisher) for 30 min. Again, the cells were rinsed with PBS and incubated with phalloidin conjugated with Alexa Fluor 488 dye (1:8000, Molecular Probes) for 20 min. Before the measurement, the cells were rinsed twice with PBS. Fluorescence images were obtained using an Olympus IX71 with a 20× air objective and were recorded and processed with Olympus CellSense software. Samples were excited with an Olympus X-Cite Q120 lamp and filtered by an Olympus U-MWIB2 filter.

2.6. Cell viability assay

Cell viability was evaluated by Trypan blue (Life Technologies). In the beginning, ECs were trypsinized, and Trypan blue (0.2%) was added to the cell suspension (at a ratio of 1:5). The prepared suspension of cells was placed on a glass slide, covered with a glass coverslip, and incubated for 3 min at RT. After this time, the set of images was performed using an optical microscope (Olympus IX71) equipped with Olympus CellSense software (version 1.41). The viable and dead cells were counted. Cell viability is presented as the percentage of viable cells in the population of cells.

2.7. Expression of E-selectin and ICAM-1

EA.hy926 cells were cultured on 24-well black plates. Cells were fixed with methanol for 5 min at −10 °C. Next, they were gently rinsed with PBS and incubated with blocking peptide solution (sc-516214, Santa Cruz Biotechnology) for 30 min. After this time, they were washed three times with PBS. For *E*-selectin staining, the cells were incubated with *E*-Selectin antibody (10 μg/mL, sc-137054, Santa Cruz Biotechnology) conjugated with Alexa Fluor 488 for 12 h. Nuclei were counterstained with Hoechst (Thermo Fisher). For ICAM-1 staining, cells were incubated with anti-ICAM-1 antibody conjugated with Alexa Fluor 488 (5 μg/mL, Santa Cruz Biotechnology) for 1 h, followed by nuclear staining with Hoechst (Thermo Fisher). The fluorescence intensity was measured using a fluorescence Microplate Reader (Infinite M200 PRO, Tecan).

2.8. Glycocalyx visualization

The cells were grown on 24-well plates and stimulated with 10 μM metformin for 72 h and 360 h. After the appropriate time, cells were fixed with paraformaldehyde (3.8%, Sigma) for 10 min. Next, cells were gently rinsed in PBS three times and incubated with blocking peptide solution (Santa Cruz Biotechnology) for 30 min. After this time, they were washed three times in PBS and incubated with biotinylated wheat germ agglutinin (WGA, Vector Laboratories) or *Maackia amurensis* lectin II (MAL II, Vector Laboratories) for 30 min. Next, cells were washed three times and incubated with avidin conjugated with Alexa Fluor 546. Cell nuclei were stained with Hoechst (Thermo Fisher). Images were taken using a Zeiss LSM710 confocal microscope and the original software by Zeiss.

2.9. Statistical analysis

The AFM nanoindentation and SCFS, as well as the fluorescence intensity data are presented in the form of box plots [the box represents the standard deviation (SD) and whiskers represent the range of the 5th to 95th percentile]. Statistical significance was tested using two-way ANOVA ($p < .05$), with independent variables being the time of incubation and sample type, i.e., control (ctr) or metformin (met). ANOVA was followed by Tukey's multiple comparison tests. Since the AFM data were log-normally distributed, we performed data transformation using a natural logarithm, in order to use the ANOVA statistical test (see Fig. S4 in Supplementary Information). This analysis was applied to all AFM data. The means (blue line in all scatter plots) of the logarithmically transformed data were then back-transformed using the procedure described by Limpert et al. [33]. In the manuscript, all data was shown as a non-transformed raw data in order to show the real spread of data points as well as the skewness of the distributions.

3. Results

3.1. Metformin attenuates cancer cell-endothelium adhesive interactions

EA.hy926 immortalized endothelial cells were selected as an experimental model because, in contrast to primary endothelial cells [34,35], they tolerate continuous culture in hyperglycemic conditions (25 mM) well. In our previous paper, we have shown that the sustained growth of EA.hy926 cells in high glucose (HG) concentrations causes a gradual increase in their stiffness [36]. Therefore, the study was carried out on the cells presenting stable elastic modulus values and nanomechanical properties (between 57 and 72 days of culture in HG) (Fig. 1A, S1D). A nontoxic concentration of metformin (10 μM) was selected for the subsequent experiments (Fig. 1B). No cytotoxic effect at this concentration was also observed for A549 cells. The effect of metformin was checked in two experimental settings. For the short-term studies, EA.hy926 cells were exposed to metformin for 72 h, of

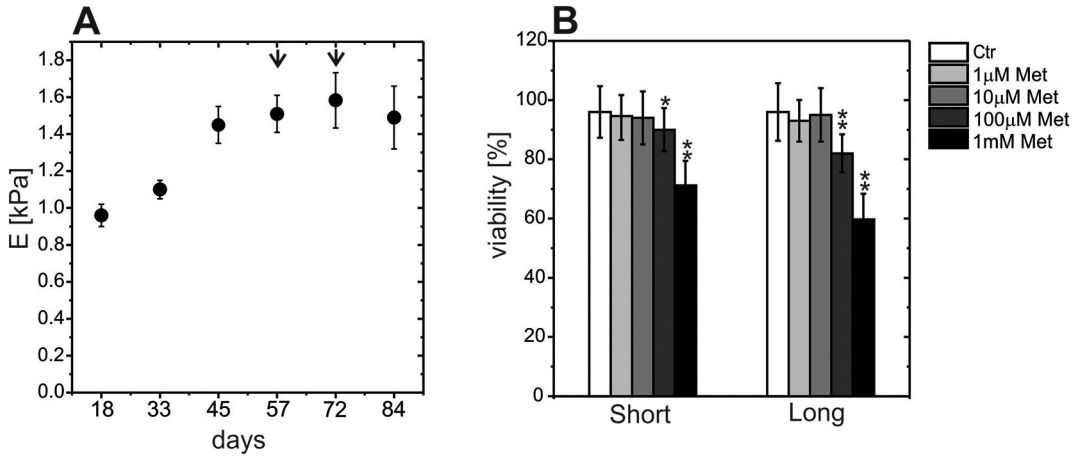

Fig. 1. Specification of the experimental model.(A) Time-dependent changes in the elastic modulus of endothelial cells growing in HG conditions. Arrows mark the time-points selected for experiments, for which stable values of the elastic modulus were observed. $n = 3$ experiments, $N = 15$ cells. **(B)** Viability assay performed for different concentrations of metformin in HG concentration. $n = 2$ experiments, $N = 40$ cells. One-way ANOVA followed by Tukey's posttest, $^{*}p < .05$, $^{**}p < .01$. Ctr – vehicle.

which 24 h were under static conditions to allow their attachment after plating and another 48 h were in laminar flow, followed by AFM measurements and other analyses, while for the long-term effects, the cells were additionally pretreated with metformin for 12 days. A549 cells were exposed to metformin in HG medium for 72 h or 15 days in static conditions.

We observed that the longer the time of EA.hy926 cell culture in HG conditions is, the stronger the adhesion interactions between cancer cells and the endothelium are (Fig. 2), as indicated by the increased total adhesion force (Fig. 2A), work of detachment (Fig. 2B) and the frequency of rupture force events (Fig. 2C). Both short- and long-term treatment of ECs and A549 cells with metformin caused a decrease in all inspected parameters (Fig. 2A-C). The total adhesion force, the work of detachment and the frequency of rupture force remained significantly increased in the group treated with metformin cultured for a longer time in HG in comparison to short-time incubation (Fig. 2). These results show that metformin can counteract adhesive interactions between ECs and cancer cells in hyperglycemic conditions. Moreover, the force and work needed for cancer cell and endothelial cell detachment are higher for the cells incubated longer in HG conditions, regardless of metformin treatment.

3.2. Metformin facilitates endothelial glycocalyx barrier regeneration

Our previous studies demonstrated that culture of ECs and cancer cells in prolonged hyperglycemic conditions causes gradual reduction of the glycocalyx layer [28]. As depicted in Fig. 3, the treatment of cells with metformin restored the glycocalyx parameters in comparison to control cells. Grafting density of the glycocalyx layer, but not its length, significantly increased in response to short-term exposure of ECs to metformin (Fig. 3A, B). Long-term treatment of ECs with metformin improved both the grafting density of the glycocalyx layer and the length of the glycocalyx brush (Fig. 3A, B). These results were fully corroborated by fluorescent imaging. Staining of ECs with wheat germ agglutinin (WGA), binding sialic acid and *N*-acetylglucosaminyl residues, which are present on ECs [37], revealed that both short- and long-term incubation of ECs with metformin increased these glycocalyx components (Fig. 3C-F, K). Additionally, binding of *Maackia amurensis* lectin II (MAL II), which recognizes sialic acid, was augmented in response to metformin treatment, regardless of the exposure time (Fig. 3G-J, L).

Moreover, firm and clearly visible actin fibres were observed for the cells cultured in HG conditions (Fig. 4A, C, E, G), in accordance with the

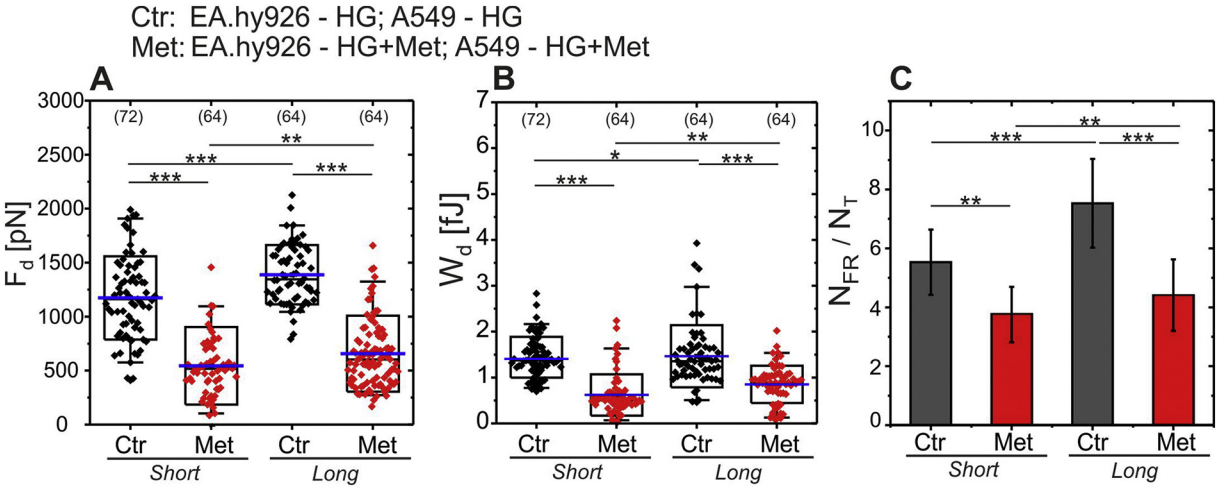

Fig. 2. Metformin attenuates the adhesive interactions between cancer cells and the endothelium. (A) Total adhesion force n = 2 experiments, $N = 8$ cells, (B) work of detachment n = 2 experiments, N = 8 cells and (C) frequency of rupture events n = 2 experiments, N = 8 cells. The numbers in brackets indicate the total number of curves taken into analysis. Two-way ANOVA followed by Tukey's posttest, $^{*}p < .05$, $^{**}p < .01$, $^{***}p < .001$. (ns) nonsignificant. Ctr – vehicle. EA.hy926 and A549 cells were cultured in HG conditions with or without 10 μM metformin.

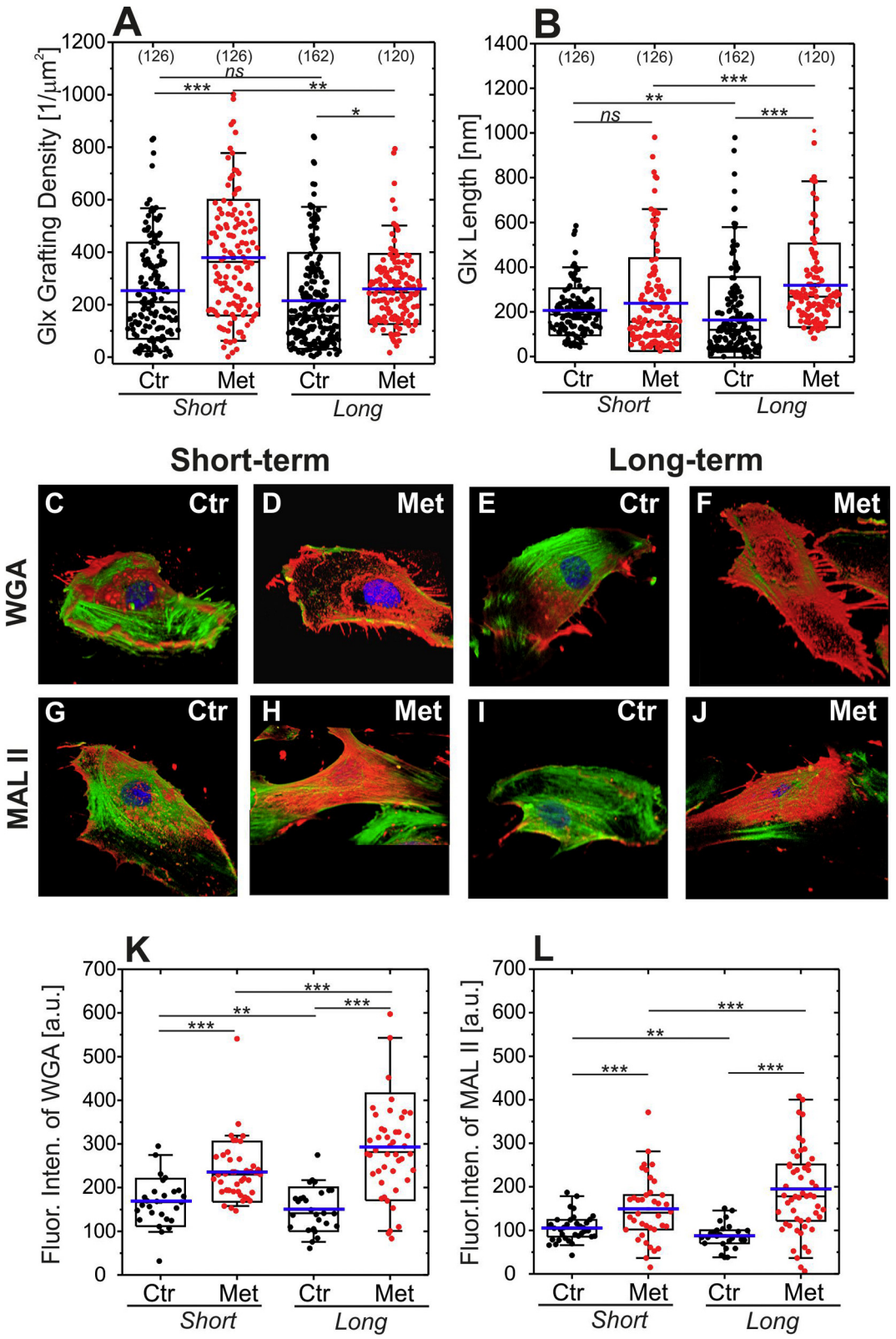

Fig. 3. Metformin induces glycocalyx restoration. (A) Glycocalyx grafting density, $n = 4$ experiments, $N = 14$ cells. (B) Length of endothelial glycocalyx layer, n = 4 experiments, N = 14 cells. Representative pictures of endothelial cells stained by WGA lectin (red)/phalloidin (green) (C–F) and MAL II lectin (red)/phalloidin (green) (G-J). Quantitative data of (K) WGA, $N = 30$ cells, and (L) MAL II, $N = 36$ cells, mean fluorescence intensity. The numbers in brackets indicate the total number of curves taken into analysis. Two-way ANOVA followed by Tukey's posttest. $^{*}p < .05$, $^{**}p < .01$, $^{***}p < .001$. (ns) nonsignificant. Ctr – vehicle. EA.hy926 cells were cultured in HG under flow conditions with or without 10 µM metformin .

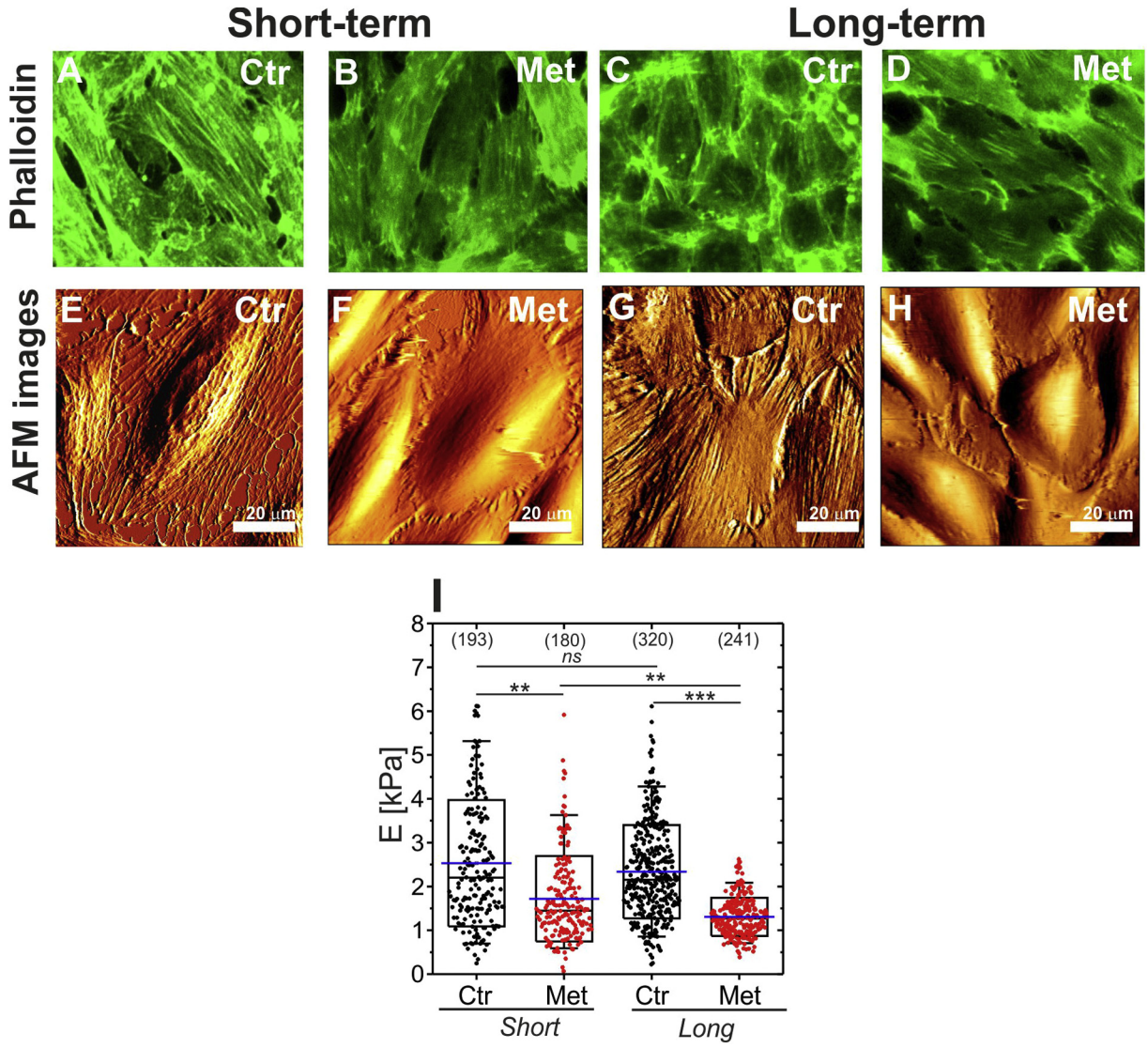

Fig. 4. Metformin reduces endothelial cell stiffness and alters actin architecture. (A-D) Representative pictures of actin fibres. *N* = 35 cells. (*E*-H) Representative pictures of AFM images of the structure of the actin cytoskeleton in the EC cortex. N = 35 cells. (I) Elastic modulus values. n = 4 experiments, N = 14 cells. The numbers in brackets indicate the total number of curves taken into analysis. Two-way ANOVA followed by Tukey's posttest. $^{*}p < .05$, $^{**}p < .01$, $^{***}p < .001$. (ns) nonsignificant. Ctr – vehicle. EA.hy926 cells were cultured in HG under flow conditions with or without 10 µM metformin.

increased cellular stiffness (Fig. 4I), which is mainly determined by the structure of the actin cytoskeleton [38]. Treatment of ECs with metformin reduced the stiffness of the cells and actin polymerization (Fig. 4B, D, F, H, I). Thus, we conclude that metformin normalizes the nanomechanical properties of endothelial cells and facilitates glycocalyx barrier reconstruction.

3.3. Cancer cell glycocalyx is modulated by metformin

In the next step, we checked whether metformin affects cancer cell glycocalyx. Glycocalyx grafting density and length were slightly decreased and increased, respectively, after 72 h-exposure of A549 cells to metformin in HG (Fig. 5A,B). In contrast to glycocalyx length, its grafting density was strongly increased by prolonged incubation of A549 cells in HG conditions, and no further metformin-induced changes were observed (Fig. 5A,B). The fluorescent visualization of the glycocalyx by WGA and MAL II lectins in A549 cells confirmed that both metformin and long-exposure to HG facilitated the coverage of the cell by glycocalyx (Fig. 5C-L). In contrast to endothelial cells (Fig. 4I), metformin increased the cancer cell stiffness (Fig. 5M). These data indicate that metformin can modulate the glycocalyx barrier and cell elasticity both in endothelial and cancer cells.

3.4. The endothelial glycocalyx impairs the adhesive interactions of ECs with cancer cells

To assess whether inhibition of EC-cancer interactions by metformin results from its effect on the endothelial or tumor cell, we performed analysis of the total adhesion force, the work of detachment, and the frequency of rupture force events between endothelial and cancer cells in the experimental setting, where ECs, but not A549 cells, were exposed to metformin. The experiments revealed that the pattern of total adhesion force, work of detachment and frequency of rapture events between the cancer cell and endothelium (Fig. 6) is similar to that seen when both cell types were stimulated with metformin (Fig. 2).

It is plausible, therefore, that metformin-induced attenuation of endothelial-cancer cell interactions is rather related to its influence on endothelial cells, but not on cancer cells. Consequently, we hypothesized that the inhibitory effects of metformin on the cancer cell-endothelium adhesive interactions are mediated by endothelial glycocalyx

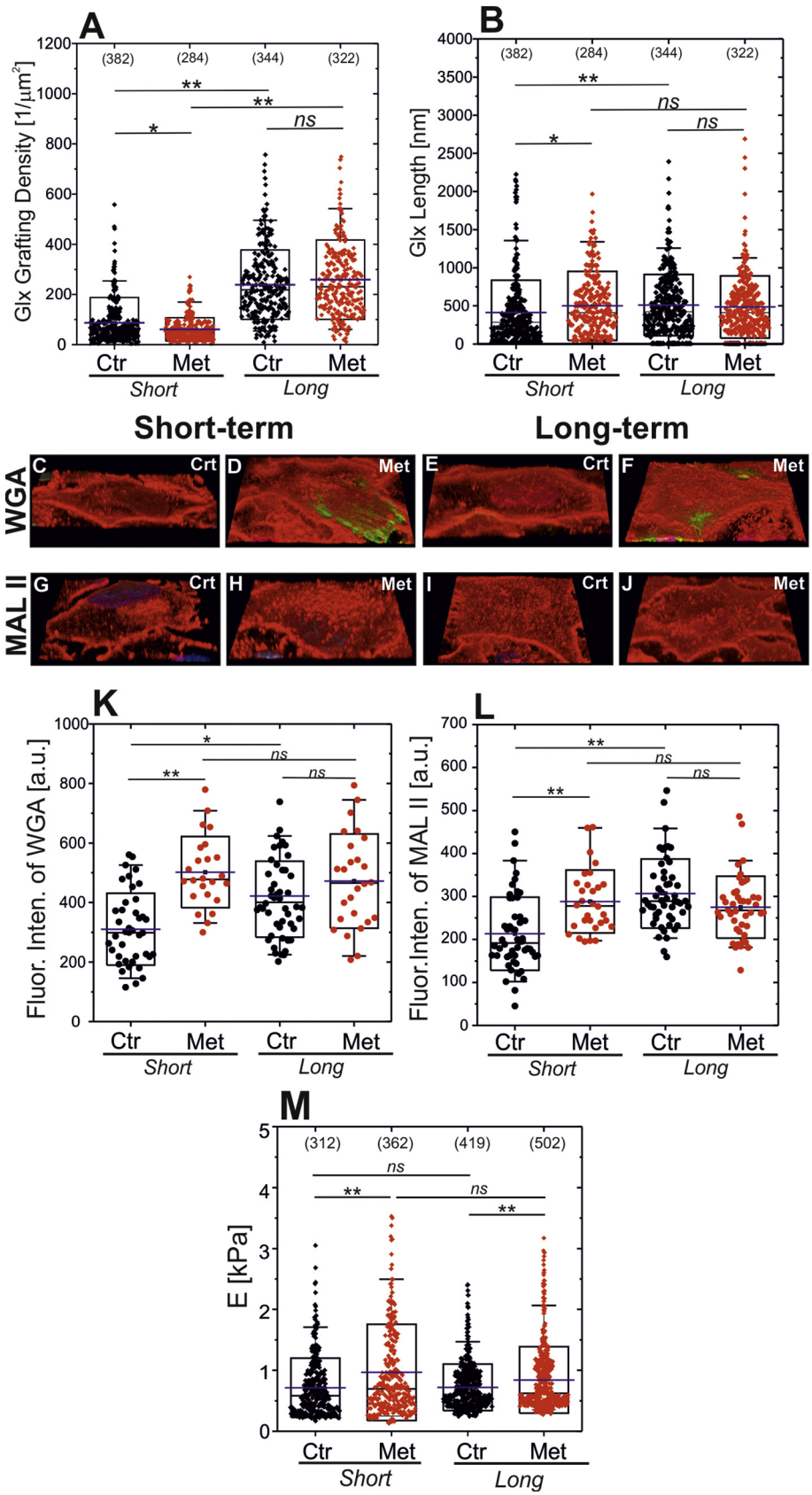

Fig. 5. Metformin affects the glycocalyx in A549 cells. (A) Glycocalyx grafting density (n = 2 experiments, N = 9 cells). (B) Length of glycocalyx layer (n = 2 experiments, N = 9 cells). Representative pictures of A549 cells stained by WGA lectin (red)/phalloidin (green) (C–F) and MAL II lectin (red)/phalloidin (green) (G-J). Quantitative data of (K) WGA (N = 36 cells), and (L) MAL II (N = 41 cells) mean fluorescence intensity. (M) Elastic modulus values. n = 2 experiments, N = 10 cells. The numbers in brackets (A,B) indicate the total number of curves taken into analysis. Two-way ANOVA followed by Tukey's posttest. *p < .05, **p < .01. (ns) nonsignificant. Ctr – vehicle. A549 cells were cultured in HG conditions with or without 10 µM metformin.

regeneration. To address this question, ECs were treated with heparinase, to selectively shed heparan sulfate from the glycocalyx, to counteract the metformin-induced recovery of the glycocalyx. The glycocalyx length (Fig. 7A) and grafting density (Fig. 7B) decreased in cells treated with heparinase. Both the total adhesion force and work of detachment between endothelial and cancer cells, as well as the

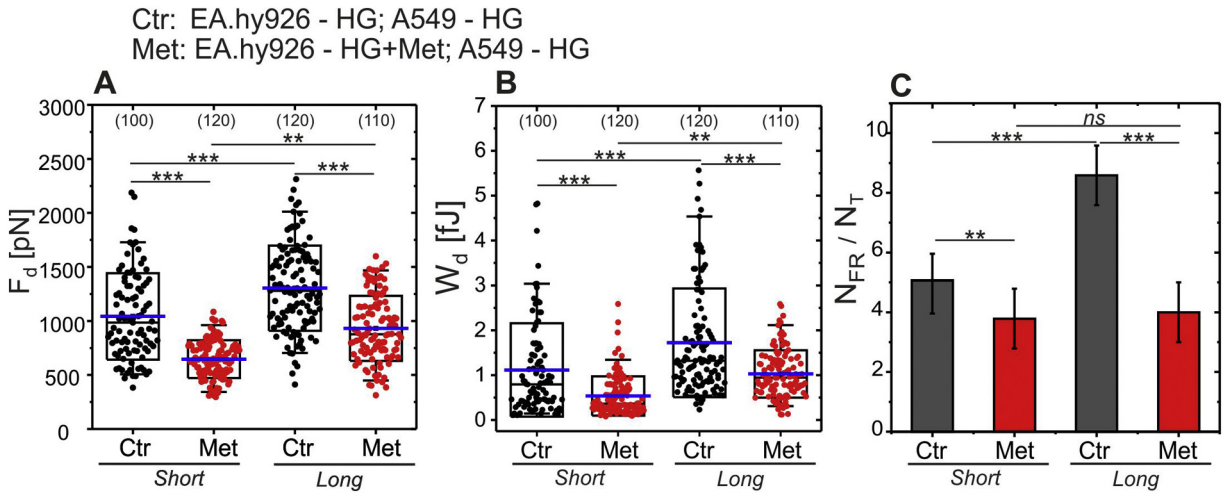

Fig. 6. Metformin attenuates adhesive interactions between the cancer cell and endothelium. (A) Total adhesion force $n = 3$ experiments, $N = 11$ cells, (B) work of detachment n = 3 experiments, N = 11 cells and (C) frequency of rupture events n = 3 experiments, N = 11 cells. Numbers in brackets indicate a total number of curves taken into analysis. Two-way ANOVA followed by Tukey's post-test, $^{*}p < .05$, $^{**}p < .01$, $^{***}p < .001$. (ns) non-significant. Ctr – vehicle. EA.hy926 cells were cultured in HG under flow conditions with or without 10 μM metformin. A549 cells were cultured in HG conditions and were not exposed to metformin.

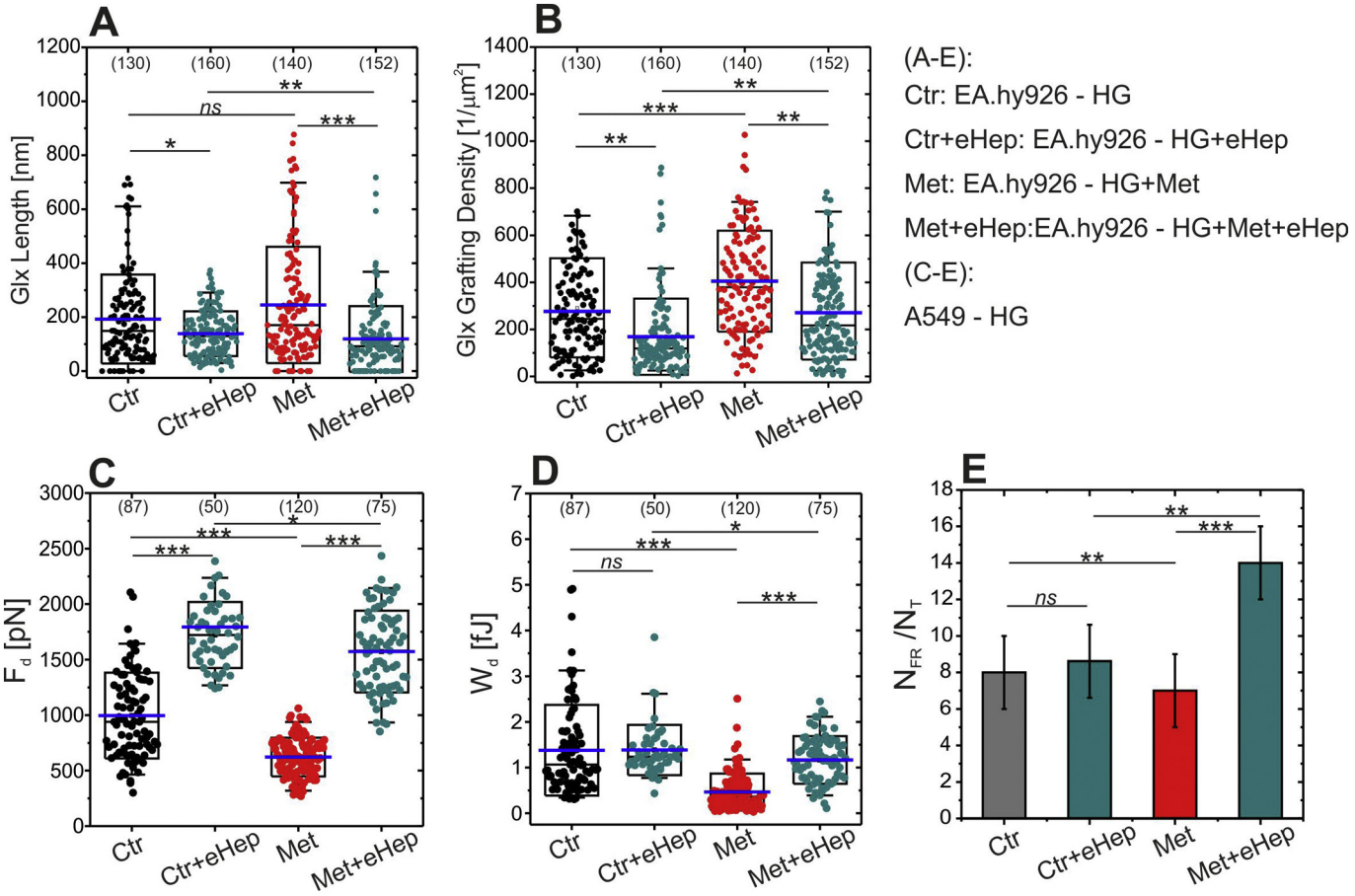

Fig. 7. Enzymatic degradation of the glycocalyx reverses the effect of metformin on the adhesive interactions between cancer cells and the endothelium. (A) Glycocalyx length, $n = 2$ experiments, $N = 10$ cells, (B) Glycocalyx grafting density, n = 2 experiments, N = 10 cells, (C) Total adhesion force, n = 2 experiments, N = 10 cells, (D) Work of detachment, n = 2 experiments, N = 10 cells. (E) Frequency of rupture events, n = 2 experiments, N = 10 cells. Numbers in brackets indicate the total number of curves considered in the analysis. Two-way ANOVA followed by Tukey's posttest. $^{*}p < .05$, $^{**}p < .01$, $^{***}p < .001$. (ns) nonsignificant. eHep – heparinase, Ctr – vehicle. EA.hy926 cells were cultured in HG under flow conditions with or without 10 μM metformin. A549 cells were cultured in HG conditions and were not exposed to metformin.

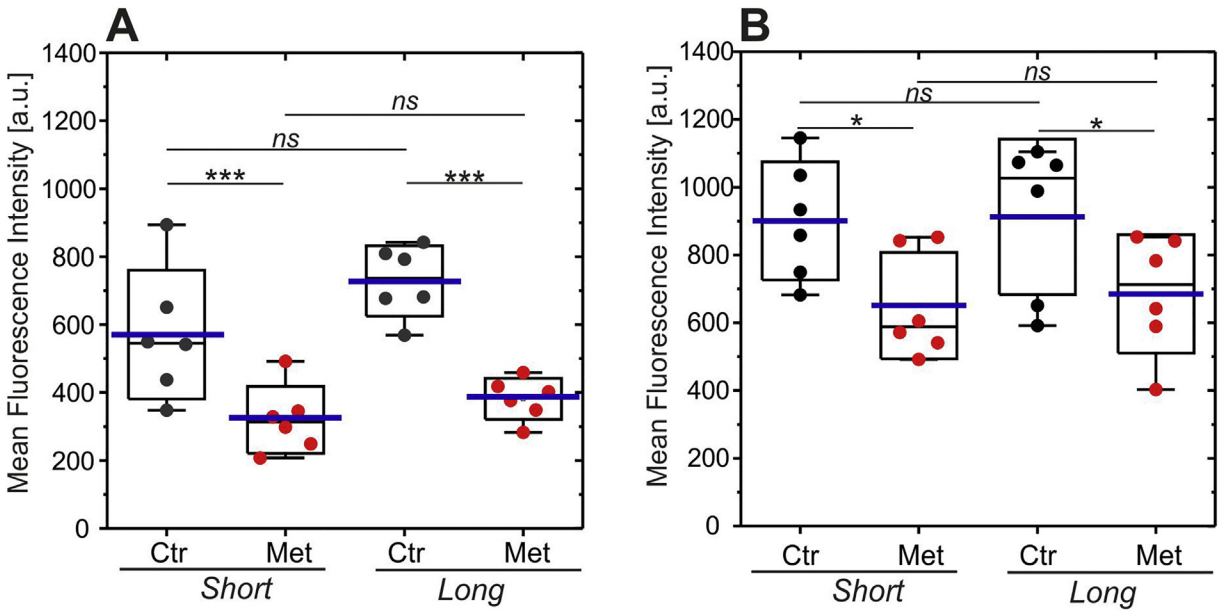

Fig. 8. Surface level of adhesion molecules on endothelial cells (A) *E*-selectin level, $n = 6$ experiments. (B) ICAM-1 level, n = 6 experiments. Two-way ANOVA followed by Tukey's posttest. $^{*}p < .05$, $^{**}p < .01$, $^{***}p < .001$. (ns) nonsignificant. EA.hy926 cells were cultured in HG conditions with or without 10 μM metformin.

frequency of rupture force events, were heavily increased in response to heparinase treatment in cells cultured in the presence of metformin (Fig. 7C-E).

These results show that metformin-stimulated regeneration of the glycocalyx may be responsible for the attenuation of cancer cell-endothelium adhesive interactions. This effect can also be facilitated by the metformin-induced downregulation of surface expression of the adhesion molecules ICAM and *E*-selectin (Fig. 8A, B) on endothelial cells. Both mechanisms may contribute to the antimetastatic effect of metformin observed in vivo.

4. Discussion

The significance of metformin as a potential anticancer therapy remains controversial because experimental studies are not entirely consistent with population-based analyses [22]. Taking into consideration the pleiotropic activity of metformin and the mechanisms that have not been fully understood yet [1], and, on the other hand, promising results of some clinical reports [22], further detailed experimental and clinical studies with a mechanistic approach are needed to obtain a clear answer regarding the anticancer potential of this drug. In light of data showing the antimetastatic properties of metformin, a decreased rate of distant metastasis and distant metastasis-free survival in comparison to non-metformin diabetic patients with prostate cancer [39], as well as inhibition of metastasis of ovarian tumors and melanoma in mice treated with metformin [23,40], we aimed to verify by direct measurement on a single cell level if metformin can inhibit cancer cell-endothelium adhesive interactions. In this study, we report that metformin attenuates the adhesion of cancer cells to the endothelium by improving the nanomechanical properties of endothelial cells, in particular by restoring the endothelial glycocalyx layer in chronic hyperglycemia. Thus, this mechanism may contribute to the antimetastatic effects of metformin.

Glycocalyx tightly covers the cell surface and shields adhesion molecules from interactions with other cells [41]. Increased exposition of membrane proteins (i.e., adhesive molecules) contributes not only to the adhesion of leukocytes but also to cancer cells [42–44]. Injury of this layer on endothelial cells in hyperglycemia was previously reported as a cause of endothelial dysfunction development [26,45,46]. Prolonged hyperglycemia results in increased surface expression of adhesion molecules, adhesive interactions with circulating cells and higher endothelial permeability for cells and molecules [47]. Accordingly, the reduction of the endothelial glycocalyx layer modulates the adhesion of cancer cells to the endothelium [28]. As we show here, treatment of endothelial cells cultured in hyperglycemic conditions with metformin reduces the total adhesion force and the work of detachment for cancer cells, which is related to changes occurring on the cell surface, including decreased surface expression of E-selectin and ICAM and reconstruction of the glycocalyx layer. As the most visible effect was noted for the glycocalyx grafting density, it seems that metformin stimulates “de novo” synthesis of glycocalyx molecules in endothelial cells. The structure of the glycocalyx and its functionality are restored in response to metformin by increasing the content of *N*-acetylglucosamine (GlcNAc) and sialic acid on the cell surface. The increase in GlcNAc content is mainly related to the structural restoration of the glycocalyx layer by reconstruction of the GAG chains [48]. However, an increase in sialic acid in the glycocalyx may influence cell function. Sialic acid is one of the terminal monosaccharides which controls vascular permeability [49]. In hyperglycemia, sialic acid is shed from the endothelial cell surface into the plasma and is regarded as a predictive biomarker of diabetic complications [50]. The molecule of sialic acid in physiological conditions is negatively ionized. Therefore, it forms a net negative charge on the cell surface, which protects endothelial cells from adhesive interactions with circulating cells [51].

The effect of metformin on endothelial glycocalyx was previously studied by Eskens et al. in db/db mice [45]. The authors have reported that metformin causes partial recovery of diabetes-associated disruption of the glycocalyx barrier and therefore regulates endothelial permeability [45], which is in accordance with studies performed on pulmonary microvascular endothelial cells [52] and in mice [44]. The literature reports that metformin alleviates endothelial dysfunction mainly by increasing NO production, inhibiting inflammatory pathways and regulating mitochondrial ROS production [2,3,53]. Our data indicate that metformin also improves the nanomechanical properties of ECs, which may affect the functionality of ECs, as endothelial stiffening is one of the symptoms of endothelial dysfunction and is related to the attenuation of NO production [54]. In contrast, the reduction of cell stiffness leads to improved endothelial function and, consequently,

increased or stabilized NO production by the endothelium [54].

5. Conclusions

In conclusion, we showed that metformin has a beneficial impact on endothelial cells and reduces the interactions between cancer cells and the endothelium in chronic hyperglycemia. Metformin improves endothelial glycocalyx properties, increases its length and grafting density and restores sialic acid and GlcNAc components, which, in turn, may inhibit the adhesive interactions of endothelial cells with cancer cells.

Funding

This research was supported by the 1.1.2 PO IG EU project POMOST FNP: “Elasticity parameter and strength of cell to cell interaction as a new marker of endothelial cell dysfunction in hyperglycemia/hypoglycemia”. DK acknowledges financial support from the National Science Centre Poland (NCN) under the ETIUDA doctoral scholarship on the basis of the decision number DEC-2019/32/T/NZ3/00326.

Authors' contributions

MTK conceived and designed the study, performed nanoindentation measurements and data analysis and wrote the manuscript; KMZ performed SCFS measurements and data analysis; DK prepared fluorescence samples; ZR performed fluorescence imaging; EŁS was involved in the discussion and contributed to the manuscript; AGP interpreted the data and wrote the manuscript; MS provided specialized AFM system, participated in discussions and commented on the manuscript. All authors read and approved the final manuscript. The authors declare no competing financial interests.

Availability of data and materials

The datasets used and analyzed in the current study are available from the corresponding author on reasonable request. In general, data generated or analyzed within this study are included in this published article.

Appendix A. Supplementary data

Supplementary data to this article can be found online at https://doi.org/10.1016/j.bbagen.2020.129533.

References

[1] A.R. Konopka, B.F. Miller, Taming expectations of metformin as a treatment to extend healthspan, GeroScience (2019), https://doi.org/10.1007/s11357-019-00057-3.
[2] B. Viollet, B. Guigas, N. Sanz Garcia, J. Leclerc, M. Foretz, F. Andreelli, Cellular and molecular mechanisms of metformin: an overview, Clin Sci Lond Engl 1979 (122) (2012) 253–270.
[3] D. Detaille, B. Guigas, C. Chauvin, C. Batandier, E. Fontaine, N. Wiernsperger, et al., Metformin prevents high-glucose-induced endothelial cell death through a mitochondrial permeability transition-dependent process, Diabetes 54 (2005) 2179–2187.
[4] G. Arunachalam, S.M. Samuel, I. Marei, H. Ding, C.R. Triggle, Metformin modulates hyperglycaemia-induced endothelial senescence and apoptosis through SIRT1, Br. J. Pharmacol. 171 (2014) 523–535.
[5] W.S. Cheang, X.Y. Tian, W.T. Wong, C.W. Lau, S.S.-T. Lee, Z.Y. Chen, et al., Metformin protects endothelial function in diet-induced obese mice by inhibition of endoplasmic reticulum stress through 5′ adenosine monophosphate-activated protein kinase-peroxisome proliferator-activated receptor δ pathway, Arterioscler. Thromb. Vasc. Biol. 34 (2014) 830–836.
[6] B.J. Davis, Z. Xie, B. Viollet, M.-H. Zou, Activation of the AMP-activated kinase by antidiabetes drug metformin stimulates nitric oxide synthesis in vivo by promoting the association of heat shock protein 90 and endothelial nitric oxide synthase, Diabetes 55 (2006) 496–505.
[7] M. Yin, I.C.C. van der Horst, J.P. van Melle, C. Qian, W.H. van Gilst, H.H.W. Silljé, et al., Metformin improves cardiac function in a nondiabetic rat model of post-MI heart failure, Am. J. Physiol. Heart Circ. Physiol. 301 (2011) H459–H468.
[8] V.N. Anisimov, L.M. Berstein, P.A. Egormin, T.S. Piskunova, I.G. Popovich, M.A. Zabezhinski, et al., Metformin slows down aging and extends life span of female SHR mice, Cell Cycle 7 (2008) 2769–2773.
[9] A. Martin-Montalvo, E.M. Mercken, S.J. Mitchell, H.H. Palacios, P.L. Mote, M. Scheibye-Knudsen, et al., Metformin improves healthspan and lifespan in mice, Nat. Commun. 4 (2013) 2192.
[10] R. Strong, R.A. Miller, A. Antebi, C.M. Astle, M. Bogue, M.S. Denzel, et al., Longer lifespan in male mice treated with a weakly estrogenic agonist, an antioxidant, an α-glucosidase inhibitor or a Nrf2-inducer, Aging Cell 15 (2016) 872–884.
[11] D.L. Smith, C.F. Elam, J.A. Mattison, M.A. Lane, G.S. Roth, D.K. Ingram, et al., Metformin supplementation and life span in Fischer-344 rats, J. Gerontol. A Biol. Sci. Med. Sci. 65 (2010) 468–474.
[12] J.M. Campbell, S.M. Bellman, M.D. Stephenson, K. Lisy, Metformin reduces all-cause mortality and diseases of ageing independent of its effect on diabetes control: a systematic review and meta-analysis, Ageing Res. Rev. 40 (2017) 31–44.
[13] Effect of intensive blood-glucose control with metformin on complications in overweight patients with type 2 diabetes (UKPDS 34), UK prospective diabetes study (UKPDS) group, Lancet Lond Engl 352 (1998) 854–865.
[14] S.J. Griffin, J.K. Leaver, G.J. Irving, Impact of metformin on cardiovascular disease: a meta-analysis of randomised trials among people with type 2 diabetes, Diabetologia 60 (2017) 1620–1629.
[15] E. Giovannucci, D.M. Harlan, M.C. Archer, R.M. Bergenstal, S.M. Gapstur, L.A. Habel, et al., Diabetes and cancer: a consensus report, Diabetes Care 33 (2010) 1674–1685.
[16] M. Jalving, J.A. Gietema, J.D. Lefrandt, J.S. de, A.K.L. Reyners, R.O.B. Gans, et al., Metformin: taking away the candy for cancer? Eur. J. Cancer 46 (2010) 2369–2380.
[17] T.Y. Ryu, J. Park, P.E. Scherer, Hyperglycemia as a risk factor for Cancer progression, Diabetes Metab. J. 38 (2014) 330–336.
[18] J.M.M. Evans, L.A. Donnelly, A.M. Emslie-Smith, D.R. Alessi, A.D. Morris, Metformin and reduced risk of cancer in diabetic patients, BMJ 330 (2005) 1304–1305.
[19] G.W.D. Landman, N. Kleefstra, K.J.J. van Hateren, K.H. Groenier, R.O.B. Gans, H.J.G. Bilo, Metformin associated with lower cancer mortality in type 2 diabetes: ZODIAC-16, Diabetes Care 33 (2010) 322–326.
[20] M. Bodmer, C. Meier, S. Krähenbühl, S.S. Jick, C.R. Meier, Long-term metformin use is associated with decreased risk of breast Cancer, Diabetes Care 33 (2010) 1304–1308.
[21] D. Li, S.-C.J. Yeung, M.M. Hassan, M. Konopleva, J.L. Abbruzzese, Antidiabetic therapies affect risk of pancreatic cancer, Gastroenterology 137 (2009) 482–488.
[22] I. Pernicova, M. Korbonits, Metformin–mode of action and clinical implications for diabetes and cancer, Nat Rev Endocrinol 10 (2014) 143–156.
[23] R. Rattan, R.P. Graham, J.L. Maguire, S. Giri, V. Shridhar, Metformin suppresses ovarian cancer growth and metastasis with enhancement of cisplatin cytotoxicity in vivo, Neoplasia N Y N 13 (2011) 483–491.
[24] N. Reymond, B.B. d'Água, A.J. Ridley, Crossing the endothelial barrier during metastasis, Nat. Rev. Cancer 13 (2013) 858–870.
[25] M.J. Mitchell, M.R. King, Physical biology in cancer. 3. The role of cell glycocalyx in vascular transport of circulating tumor cells, Am J Physiol Cell Physiol 306 (2014) C89–C97.
[26] M. Nieuwdorp, T.W. van Haeften, M.C.L.G. Gouverneur, H.L. Mooij, M.H.P. van Lieshout, M. Levi, et al., Loss of endothelial glycocalyx during acute hyperglycemia coincides with endothelial dysfunction and coagulation activation in vivo, Diabetes 55 (2006) 480–486.
[27] D. Chappell, N. Dörfler, M. Jacob, M. Rehm, U. Welsch, P. Conzen, et al., Glycocalyx protection reduces leukocyte adhesion after ischemia/reperfusion, Shock Augusta Ga 34 (2010) 133–139.
[28] K.E. Malek-Zietek, M. Targosz-Korecka, M. Szymonski, The impact of hyperglycemia on adhesion between endothelial and cancer cells revealed by single-cell force spectroscopy, J Mol Recognit JMR 30 (2017), https://doi.org/10.1002/jmr.2628.
[29] J. Helenius, C.-P. Heisenberg, H.E. Gaub, D.J. Muller, Single-cell force spectroscopy, J. Cell Sci. 121 (2008) 1785–1791.
[30] C. Mousoulis, X. Xu, D.A. Reiter, C.P. Neu, Single cell spectroscopy: noninvasive measures of small-scale structure and function, Methods San Diego Calif 64 (2013) 119–128.
[31] I. Sokolov, M.E. Dokukin, N.V. Guz, Method for quantitative measurements of the elastic modulus of biological cells in AFM indentation experiments, Methods San Diego Calif 60 (2013) 202–213.
[32] N. Guz, M. Dokukin, V. Kalaparthi, I. Sokolov, If cell mechanics can be described by elastic modulus: study of different models and probes used in indentation experiments, Biophys. J. 107 (2014) 564–575.
[33] E. Limpert, W.A. Stahel, M. Abbt, Log-normal distributions across the sciences: keys and CluesOn the charms of statistics, and how mechanical models resembling gambling machines offer a link to a handy way to characterize log-normal distributions, which can provide deeper insight into variability and probability—normal or log-normal: that is the question, BioScience 51 (2001) 341–352.
[34] R. Ambra, S. Manca, M.C. Palumbo, G. Leoni, L. Natarelli, A. De Marco, et al., Transcriptome analysis of human primary endothelial cells (HUVEC) from umbilical cords of gestational diabetic mothers reveals candidate sites for an epigenetic modulation of specific gene expression, Genomics 103 (2014) 337–348.
[35] S. Karbach, T. Jansen, S. Horke, T. Heeren, A. Scholz, M. Coldewey, et al., Hyperglycemia and oxidative stress in cultured endothelial cells–a comparison of primary endothelial cells with an immortalized endothelial cell line, J. Diabetes Complicat. 26 (2012) 155–162.
[36] M. Targosz-Korecka, G.D. Brzezinka, K.E. Malek, E. Stępień, M. Szymonski, Stiffness memory of EA.hy926 endothelial cells in response to chronic hyperglycemia,

Cardiovasc. Diabetol. 12 (2013) 96.
[37] A.R. Pries, T.W. Secomb, P. Gaehtgens, The endothelial surface layer, Pflugers Arch. 440 (2000) 653–666.
[38] M. Targosz-Korecka, K.E. Malek-Zietek, G.D. Brzezinka, M. Jaglarz, Morphological and nanomechanical changes in mechanosensitive endothelial cells induced by colloidal AFM probes, Scanning 38 (2016) 654–664.
[39] D.E. Spratt, C. Zhang, Z.S. Zumsteg, X. Pei, Z. Zhang, M.J. Zelefsky, Metformin and prostate cancer: reduced development of castration-resistant disease and prostate cancer mortality, Eur. Urol. 63 (2013) 709–716.
[40] M. Cerezo, M. Tichet, P. Abbe, M. Ohanna, A. Lehraiki, F. Rouaud, et al., Metformin blocks melanoma invasion and metastasis development in AMPK/p53-dependent manner, Mol. Cancer Ther. 12 (2013) 1605–1615.
[41] A.W. Mulivor, H.H. Lipowsky, Role of glycocalyx in leukocyte-endothelial cell adhesion, Am. J. Physiol. Heart Circ. Physiol. 283 (2002) H1282–H1291.
[42] H.H. Lipowsky, The endothelial glycocalyx as a barrier to leukocyte adhesion and its mediation by extracellular proteases, Ann. Biomed. Eng. 40 (2012) 840–848.
[43] M. Morigi, S. Angioletti, B. Imberti, R. Donadelli, G. Micheletti, M. Figliuzzi, et al., Leukocyte-endothelial interaction is augmented by high glucose concentrations and hyperglycemia in a NF-kB-dependent fashion, J. Clin. Invest. 101 (1998) 1905–1915.
[44] E.P. Schmidt, Y. Yang, W.J. Janssen, A. Gandjeva, M.J. Perez, L. Barthel, et al., The pulmonary endothelial glycocalyx regulates neutrophil adhesion and lung injury during experimental sepsis, Nat. Med. 18 (2012) 1217–1223.
[45] B.J.M. Eskens, C.J. Zuurbier, J. van Haare, H. Vink, J.W.G.E. van Teeffelen, Effects of two weeks of metformin treatment on whole-body glycocalyx barrier properties in db/db mice, Cardiovasc. Diabetol. 12 (2013) 175.
[46] R.M. Perrin, S.J. Harper, D.O. Bates, A role for the endothelial glycocalyx in regulating microvascular permeability in diabetes mellitus, Cell Biochem. Biophys. 49 (2007) 65–72.
[47] F. Haubner, K. Lehle, D. Münzel, C. Schmid, D.E. Birnbaum, J.G. Preuner, Hyperglycemia increases the levels of vascular cellular adhesion molecule-1 and monocyte-chemoattractant-protein-1 in the diabetic endothelial cell, Biochem. Biophys. Res. Commun. 360 (2007) 560–565.
[48] L.N. Broekhuizen, B.A. Lemkes, H.L. Mooij, M.C. Meuwese, H. Verberne, F. Holleman, et al., Effect of sulodexide on endothelial glycocalyx and vascular permeability in patients with type 2 diabetes mellitus, Diabetologia 53 (2010) 2646–2655.
[49] K.B. Betteridge, K.P. Arkill, C.R. Neal, S.J. Harper, R.R. Foster, S.C. Satchell, et al., Sialic acids regulate microvessel permeability, revealed by novel in vivo studies of endothelial glycocalyx structure and function, J. Physiol. 595 (2017) 5015–5035.
[50] P. Prajna, J.A. Kumar, S. Rai, S.K. Shetty, T. Rai, Shrinidhi null et al. Predictive value of serum sialic Acid in type-2 diabetes mellitus and its complication (nephropathy), J Clin Diagn Res JCDR 7 (2013) 2435–2437.
[51] Y. Abe, C.W. Smith, J.P. Katkin, L.M. Thurmon, X. Xu, L.H. Mendoza, et al., Endothelial alpha 2,6-linked sialic acid inhibits VCAM-1-dependent adhesion under flow conditions, J Immunol Baltim Md 1950 (163) (1999) 2867–2876.
[52] M.-Y. Jian, M.F. Alexeyev, P.E. Wolkowicz, J.W. Zmijewski, J.R. Creighton, Metformin-stimulated AMPK-α1 promotes microvascular repair in acute lung injury, Am J Physiol Lung Cell Mol Physiol 305 (2013) L844–L855.
[53] C.R. Triggle, H. Ding, Metformin is not just an antihyperglycaemic drug but also has protective effects on the vascular endothelium, Acta Physiol Oxf Engl 219 (2017) 138–151.
[54] A.M. Szczygiel, G. Brzezinka, M. Targosz-Korecka, S. Chlopicki, M. Szymonski, Elasticity changes anti-correlate with NO production for human endothelial cells stimulated with TNF-α, Pflugers Arch. 463 (2012) 487–496.